



Cite this: DOI: 10.1039/d5fo02470f

## Multi-organ ionomics elucidates the disruption of mineral homeostasis induced by zinc deficiency

Mengxu Wang,<sup>†,a</sup> Yongzhi Sun,<sup>†,b,c</sup> Yongzhu Pan,<sup>a</sup> Xinxin Gu,<sup>a</sup> Yiwen Yang,<sup>a</sup> Jingmin Tong, Lan Zhao,<sup>\*,d</sup> Ying Li <sup>\*,a</sup> and Maoqing Wang <sup>\*,a,b,c</sup>

The impact of zinc deficiency on systemic mineral homeostasis remains unclear. This study investigated the effects of zinc deficiency on mineral homeostasis by quantifying sixteen minerals across nineteen tissues, along with their intake, excretion, and distribution. Principal component analysis revealed distinct differences in the mineral composition profiles of serum, whole blood, heart, spleen, testis, urine, and feces between the low-zinc and normal-zinc diet groups. Specifically, zinc deficiency enhanced intestinal absorption of Ca, Co, V, Ni, and Mo, and decreased their excretion, leading to elevated concentrations in the blood, heart, kidneys, testes, and cecal contents. Conversely, zinc deficiency increased the excretion of As, Mg, Se, and K, resulting in reduced concentrations of these minerals in the kidneys, testes, spleen, and femur. Additionally, zinc deficiency directly influenced the distribution of Mn, Cr, Cu, Na, and Pb, causing significant alterations in their concentrations across multiple tissues. Correlation analysis revealed that changes in mineral concentrations may contribute to a spectrum of adverse health outcomes. Our findings revealed that zinc deficiency disrupts systemic mineral homeostasis through four key pathways: intake, absorption, distribution, and excretion.

Received 8th June 2025,  
Accepted 11th December 2025

DOI: 10.1039/d5fo02470f

[rsc.li/food-function](http://rsc.li/food-function)

## 1. Introduction

Zinc is an essential trace mineral required by the human body. Approximately 10% of proteins rely on zinc as a structural component or enzymatic cofactor.<sup>1</sup> Zinc deficiency can result in a spectrum of health issues, including growth retardation, impaired taste and smell, skin lesions, and compromised immune and reproductive functions.<sup>2,3</sup> An estimated 15% of the global population is affected by zinc deficiency, particularly in low- and middle-income countries, due to inadequate dietary zinc intake or poor absorption.<sup>4,5</sup>

Studies have demonstrated that zinc deficiency alters the concentrations of zinc, calcium, copper, iron, magnesium, selenium, and potassium in various tissues, including serum, liver, kidney, testis, intestine, stomach, pancreas, and prostate.<sup>6-14</sup> This mineral homeostasis imbalance can lead to

multi-level physiological and metabolic disorders, contributing to the development of various complex diseases.<sup>15,16</sup> Therefore, understanding the effects of zinc deficiency on the body's mineral homeostasis is critical.

The concentrations of minerals in the body are regulated by multiple factors, including dietary intake, absorption, excretion, and tissue distribution. Research indicates that zinc deficiency reduces food intake,<sup>17,18</sup> impairs copper and iron absorption,<sup>19,20</sup> and alters the excretion of calcium, sodium, and magnesium.<sup>9,21</sup> In our previous study, rats subjected to a low-zinc diet for 4 weeks exhibited reduced bone mineral density, decreased calcium excretion, and lower liver calcium concentration; however, serum and skeletal muscle calcium concentrations were elevated.<sup>13,22</sup> These findings suggest that zinc deficiency may induce calcium redistribution within the body. Overall, zinc deficiency likely affects mineral concentrations in tissues by influencing multiple pathways such as intake, absorption, excretion, and distribution. Therefore, identifying the causes of changes in mineral concentrations is challenging when studying only a single pathway. Current research primarily focuses on alterations in the concentrations of specific minerals (such as zinc, copper, and iron) in selected tissues<sup>6-14</sup> but lacks comprehensive investigations that assess all tissues and organs while simultaneously considering multiple pathways, including intake, absorption, excretion, and distribution. Consequently, the overall effects of zinc deficiency on systemic mineral homeostasis remain incompletely understood.

<sup>a</sup>Department of Nutrition and Food Hygiene, School of Public Health, Key Laboratory of Precision Nutrition and Health, Ministry of Education, Harbin Medical University, 157 Baofian Road, Nangang District, Heilongjiang, 150081, China.

E-mail: wang\_maoging@126.com, liying\_helen@163.com; Fax: (+86)-451-87502885; Tel: (+86)-451-87502876

<sup>b</sup>Department of Cardiology, Second Affiliated Hospital of Harbin Medical University, China

<sup>c</sup>The Key Laboratory of Myocardial Ischemia, Chinese Ministry of Education, China

<sup>d</sup>Public Health Inspection Office, Heilongjiang Center of Disease Control and Prevention, Harbin, China. E-mail: zhaolan75@163.com

<sup>†</sup>Contributed equally.



In this study, we measured the concentrations of sixteen minerals in nineteen different tissues and biological samples from zinc-deficient rats, including serum, urine, feces, and a comprehensive range of tissues and organs. We also quantified the intake and excretion of these minerals. Using these data, we investigated the effects of zinc deficiency on mineral homeostasis through multiple pathways, including intake, absorption, excretion, and distribution. Additionally, we analyzed the correlations between altered mineral levels and serum biochemical markers.

## 2. Materials and methods

### 2.1. Animal experiments

Forty-eight male Sprague-Dawley rats (4 weeks old) were randomly assigned to one of three groups: a low-zinc diet group (LZG; 10 mg kg<sup>-1</sup> zinc,  $n = 16$ ), a normal-zinc diet group (NZG; 30 mg kg<sup>-1</sup> zinc,  $n = 16$ ), and a pair-fed group (PZG; 30 mg kg<sup>-1</sup> zinc,  $n = 16$ ). The animal diets were commercial AIN-93M-based formulations (Beijing Keao Co., Ltd). To reduce zinc content, casein was replaced with egg white protein as the primary protein source. While lower in zinc than casein, egg white, together with other components (corn starch, soybean oil, fiber), still contributed trace amounts of zinc.<sup>13</sup> The composition profiles and content of each dietary mineral are detailed in Table S1. The low-zinc diet was formulated without zinc supplementation and had a measured zinc content of 10.4 mg kg<sup>-1</sup>. By adding zinc carbonate to this base diet, a normal-zinc diet targeting 30 mg kg<sup>-1</sup> was prepared; the experimentally measured value was confirmed to be 30.4 mg kg<sup>-1</sup> (Table S2). The LZG was fed a low-zinc diet, while the NZG received a normal-zinc diet. The daily food consumption of the LZG was recorded, and an equivalent amount was subsequently provided to the PZG the following day. Any remaining or wasted food was measured and accounted for on a daily basis, thereby maintaining consistent intake between the two groups under pair-fed conditions. All rats were housed individually in stainless steel cages with free access to deionized water under controlled environmental conditions (24 ± 1 °C, 50% ± 5% relative humidity, and a 12-hour light/dark cycle). The experiment was terminated when 50% of the rats in any group had died naturally. All procedures adhered to the Guide for the Care and Use of Laboratory Animals of Harbin Medical University (Harbin, China) and were approved by the Animal Ethics Committee of Harbin Medical University (HMUIRB2019007PRE).

### 2.2. Sample collection and measurement of serum biochemical indices

Before the end of the animal experiment, 48-hour urine and fecal samples were collected. The rats were fasted for 12 hours prior to euthanasia, and body weight was recorded. Blood was collected using two types of tubes: plain tubes (Labtub, China) for serum preparation and EDTA-K2 anticoagulant tubes (Labtub, China) for whole blood analysis. For serum separation, samples in plain tubes were allowed to clot at room temperature for 30 minutes, followed by centrifugation at

3000g for 15 minutes. The supernatant serum was then aliquoted and stored at -80 °C until further analysis. For whole blood samples collected in EDTA-K2 tubes, the tubes were gently inverted several times to ensure proper mixing. Aliquoting was completed within 2 hours of collection, and samples were stored at -80 °C until analysis. To exclude potential interference from EDTA-K2 in mineral analysis, we set up a matrix blank control: ultrapure water (18.2 MΩ cm) was added to the EDTA-containing anticoagulant blood collection tubes and processed alongside the samples. The measurement results of all whole blood samples were corrected by subtracting the background values from the blank control, confirming that the anticoagulant did not introduce any contamination. During tissue collection, all tissues were thoroughly rinsed with physiological saline, and the heart was perfused prior to sampling to minimize residual blood and its potential impact on mineral concentration measurements.

Serum concentrations of alanine aminotransferase (ALT), aspartate aminotransferase (AST), total cholesterol (TC), triglycerides (TG), high-density lipoprotein cholesterol (HDL-C), and low-density lipoprotein cholesterol (LDL-C) were measured using an automatic biochemical analyzer (Hitachi 7100, Japan).

### 2.3. Sample pretreatment

All samples were pretreated using a microwave digestion system (LabTech, Italy). For each sample, 100 mg of tissue (or 100 μL for serum, blood, and urine) was accurately weighed into a microwave digestion vessel. Six milliliters of concentrated nitric acid (≥65%, GR grade, Merck, Germany) were added, and digestion was performed according to the instrument's standard protocol: 150 °C for 20 minutes after a 5-minute warm-up, followed by 190 °C for 20 minutes after a 10-minute warm-up. After digestion, samples were deacidified at 160 °C, diluted to a fixed volume with deionized water (Milli-Q system, 18.2 MΩ cm), vortexed, and filtered for further analysis. The measured concentrations were normalized to tissue weight.

### 2.4. Quantification of twenty-one minerals by ICP-MS

The concentrations of twenty-one minerals in nineteen types of rat samples were determined using a Thermo Scientific iCAP-Q inductively coupled plasma mass spectrometer (ICP-MS) at the Heilongjiang Provincial Center for Disease Control and Prevention. Prior to formal analysis, tuning solutions containing Li, Y, Ce, and Tl were used to optimize the ICP-MS detection conditions. During analysis, an internal standard mixture (100 μg L<sup>-1</sup>), including Sc<sup>45</sup>, Ge<sup>72</sup>, Rh<sup>103</sup>, Tb<sup>159</sup>, Lu<sup>172</sup>, and Bi<sup>209</sup>, was introduced to correct for matrix interference. Mineral concentrations were quantified using the external calibration method, with calibration standards (Catalog No. 5183-4688) purchased from Agilent Technologies. The calibration range for each mineral was determined based on its concentration in the samples.

### 2.5. Method validation

The accuracy, recovery, and precision of the method were validated according to the aforementioned pretreatment and quantification procedures. Accuracy evaluation: the certified



reference material Seronorm Serum L-1 RUO was used for measurement, and the obtained values were compared with the certified values. Recovery evaluation: blank samples were spiked with mixed standard solutions at different concentrations. Specifically, 5% nitric acid was divided into four portions, and three portions were spiked with low, medium, and high concentrations of the target elements. The spiking concentrations for K, Ca, Na, Mg, and Fe were 1, 5, and 20 mg L<sup>-1</sup>, while those for V, Cr, Mn, Co, Ni, Cu, Zn, As, Se, Mo, and Pb were 10, 50, and 200 µg L<sup>-1</sup>. Six replicates were prepared for each concentration level. Additionally, six replicates of unspiked blank samples were measured to determine the baseline concentration. The recovery rate was calculated using the following formula: Recovery (%) = [(concentration after spiking - unspiked concentration)/spiked concentration] × 100%. Precision evaluation: three concentration levels within the standard curve range were selected. Each level was analyzed in six replicates, and the relative standard deviation (RSD) was calculated.

## 2.6. ICP-MS stability evaluation

The mixed test solution was used as a quality control (QC) sample, and one QC sample was inserted after every 30 test samples. After the experiment, principal component analysis (PCA) was performed on the measurement results to assess the stability of the instrument throughout the analytical process.

## 2.7. Data processing and analysis

Data analysis was conducted using GraphPad Prism (version 9, CA, USA) and MetaboAnalyst 6.0 (<https://www.metaboanalyst.ca>). Results are expressed as mean ± standard deviation (SD). One-way ANOVA with the LSD *post hoc* test was used to analyze statistical differences among groups, while comparisons between two groups were performed using the *t*-test. The Ward method, with Euclidean distance as the distance metric, was applied for sample clustering. Principal component analysis (PCA), combined with multivariate analysis of variance (MANOVA), was employed to assess differences in mineral composition profiles across tissue groups. The Spearman rank correlation coefficient was used to evaluate correlations between mineral concentrations in each organ and serum biochemical markers. The 24-hour *in vitro* excretion of each mineral was calculated as follows: Mineral excretion = (mineral concentration in urine × urine volume) + (mineral concentration in feces × fecal excretion). The apparent absorption rate for each mineral was calculated as follows: (Mineral intake - total mineral excretion)/mineral intake × 100%. All statistical tests were two-tailed, and a *P*-value < 0.05 was considered statistically significant.

## 3. Results

### 3.1. Food intake, body weight, serum zinc concentration, and biochemical indices of rats

At the end of the experiment, the median survival time—defined as the age at which half of the animals in a group had

died—was 23 months for the NZG, and approximately 25 months for both the LZG and PZG. The average food intake during the final month showed no significant differences among the groups (Table 1 and Fig. S1). Compared to the NZG and PZG, serum zinc concentration was significantly lower in the LZG (*P* < 0.05). Notably, the body weight of LZG rats did not decrease but rather demonstrated an increasing trend, a finding that warrants further investigation. Serum levels of ALT, AST, and LDL-C were significantly higher in the LZG compared to the NZG and PZG. Urine volume and fecal output showed no significant differences among the three groups (Fig. S2). No significant differences were observed between the PZG and NZG (Table 1).

### 3.2. Method validation and instrument stability evaluation

Mineral concentrations were measured in a total of 707 samples, including feces, urine, cecal contents, femur, serum, and fourteen types of *in vivo* rat tissues. Five minerals (Al, Ag, Cd, Sb, and Ba) were omitted from further analysis due to their concentration levels being insufficient for reliable quantification, falling below the instrument's detection limit. All remaining minerals exhibited excellent linearity over their respective concentration ranges, with *R*<sup>2</sup> values consistently exceeding 0.9984 (Table S3). The analytical method demonstrated robust performance characteristics, including high accuracy, recovery rates ranging from 78.4% to 110.8%, and precision with relative standard deviations (RSD) below 7.74% (Tables S4–S6). Additionally, quality control (QC) samples exhibited tight clustering in the principal component analysis (PCA) score plot (Fig. S3), reflecting consistent instrumental performance and stability throughout the experimental procedure. These results collectively validate the reliability and reproducibility of the methodological approach employed in this study.

### 3.3. Characteristics of mineral composition profiles in rat tissues and samples

The mineral composition profiles of feces, urine, cecal contents, femur, serum, and 14 *in vivo* tissues exhibited distinct separation (Fig. 1A). Except for the duodenum and cecum, samples from the same tissue clustered together in the PCA plot (Fig. 1B)

**Table 1** Food intake, body weight, serum zinc concentration, and serum biochemical indicators of rats

	LZG	NZG	PZG
Food intake (g day <sup>-1</sup> )	22.29 ± 5.14	22.19 ± 4.69	
Body weight (g)	827.17 ± 219.33	753.63 ± 166.60	773.08 ± 79.89
Serum zinc (µg ml <sup>-1</sup> )	1.29 ± 0.28*	1.65 ± 0.30	1.56 ± 0.22
ALT (U L <sup>-1</sup> )	109.40 ± 44.75*	65.56 ± 37.40	68.20 ± 35.86
AST (U L <sup>-1</sup> )	308.33 ± 115.55*	216.22 ± 73.72	223.4 ± 103.06
TCHO (mmol L <sup>-1</sup> )	2.28 ± 0.62	1.97 ± 0.30	2.04 ± 0.66
TG (mmol L <sup>-1</sup> )	0.35 ± 0.13	0.27 ± 0.10	0.46 ± 0.28
HDL-C (mmol L <sup>-1</sup> )	0.93 ± 0.32	0.84 ± 0.20	0.85 ± 0.27
LDL-C (mmol L <sup>-1</sup> )	1.06 ± 0.40*	0.6 ± 0.14	0.73 ± 0.32

LZG: low-zinc group; NZG: normal-zinc diet group; PZG: pair-fed group. The food intake of the PZG was matched to that of the LZG. \*: *P* < 0.05 (One-way ANOVA, LZG vs. NZG and PZG).



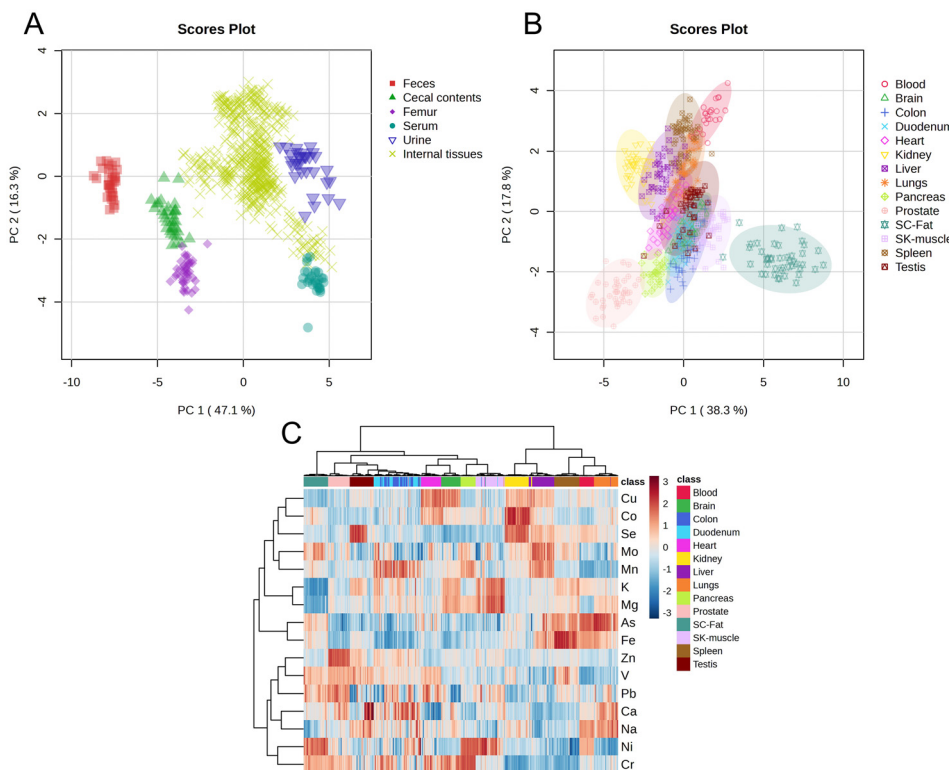


**Fig. 1** Mineral composition profiles across nineteen distinct tissues and biological samples. The results shown in (A–C) were derived from the combined data of all three groups (NZG, LZG, and PZG). (A) PCA score plot of feces, cecal contents, femur, serum, urine, and fourteen *in vivo* tissues. (B) PCA score plot of fourteen *in vivo* tissue samples. SC-Fat: subcutaneous fat; SK-muscle: skeletal muscle. (C) Heatmap showing hierarchical clustering of minerals in fourteen *in vivo* tissues. Each row corresponds to a mineral, and each column corresponds to a biological sample, with color coding consistent with (B). Hierarchical clustering was performed using the Pearson correlation coefficient as the distance measure and the Ward method as the clustering algorithm. The values shown in the heatmap range approximately from -3 to 3 and represent normalized mineral concentration data.

and were grouped into the same category in the heatmap analysis (Fig. 1C). The concentrations of 16 minerals demonstrated marked variability across the 14 *in vivo* tissues (Fig. 1C). These findings collectively underscore the complexity of mineral metabolism and its tissue-specific regulation, emphasizing the need for a comprehensive, multi-tissue approach to understanding mineral homeostasis in physiological systems.

#### 3.4. Analysis of inter-group differences in sixteen minerals among nineteen distinct tissues or samples

As shown in Fig. 2A, the mineral composition profiles of seven tissues (feces, urine, serum, whole blood, heart, spleen, and testis) in the LZG demonstrated clear separation from those of the NZG and PZG, while no significant differences were observed between the NZG and PZG. These findings suggest that zinc deficiency selectively altered the mineral composition profiles of these seven tissues, indicating their heightened sensitivity to zinc deficiency. Specifically, the concentrations of fifteen minerals (excluding Fe) were significantly altered in these tissues (Fig. 3, Tables S7–S13).

As shown in Fig. 2B, no significant inter-group variations in mineral composition profiles were detected across ten tissues (cecal contents, kidney, femur, liver, lung, skeletal muscle,

subcutaneous fat, prostate, pancreas, and brain) among the three groups. However, significant changes in the concentrations of one or more of these eleven minerals (Zn, Ca, Co, V, Ni, As, Mg, Se, K, Mn, and Cu) were observed in specific tissues (Fig. 3, Tables S14–S23).

As shown in Fig. 2C, no significant differences were observed in the mineral composition profiles of the duodenum and colon, nor in the concentrations of the sixteen minerals in these tissues (Fig. 3, Tables S24 and S25).

#### 3.5. Correlation analysis between mineral levels and serum biochemical results

As shown in Fig. 4, significant correlations were observed between one or more of the minerals (Na, Mg, K, Ca, V, Fe, Co, Zn, Se, and Mo) in tissues such as the liver, colon, heart, and spleen and the levels of ALT and AST. In the cecal contents, serum, lung, heart, liver, spleen, and other tissues, one or more of the sixteen minerals showed significant correlations with TCHO, TG, HDL-C, and LDL-C. Of particular interest, zinc deficiency markedly altered the concentrations of Na, Mg, K, Ca, V, Co, Ni, Zn, and Mo in the heart, liver, feces, urine, and other tissues (Fig. 3). These changes were significantly associated with increased ALT, AST, and LDL-C levels.

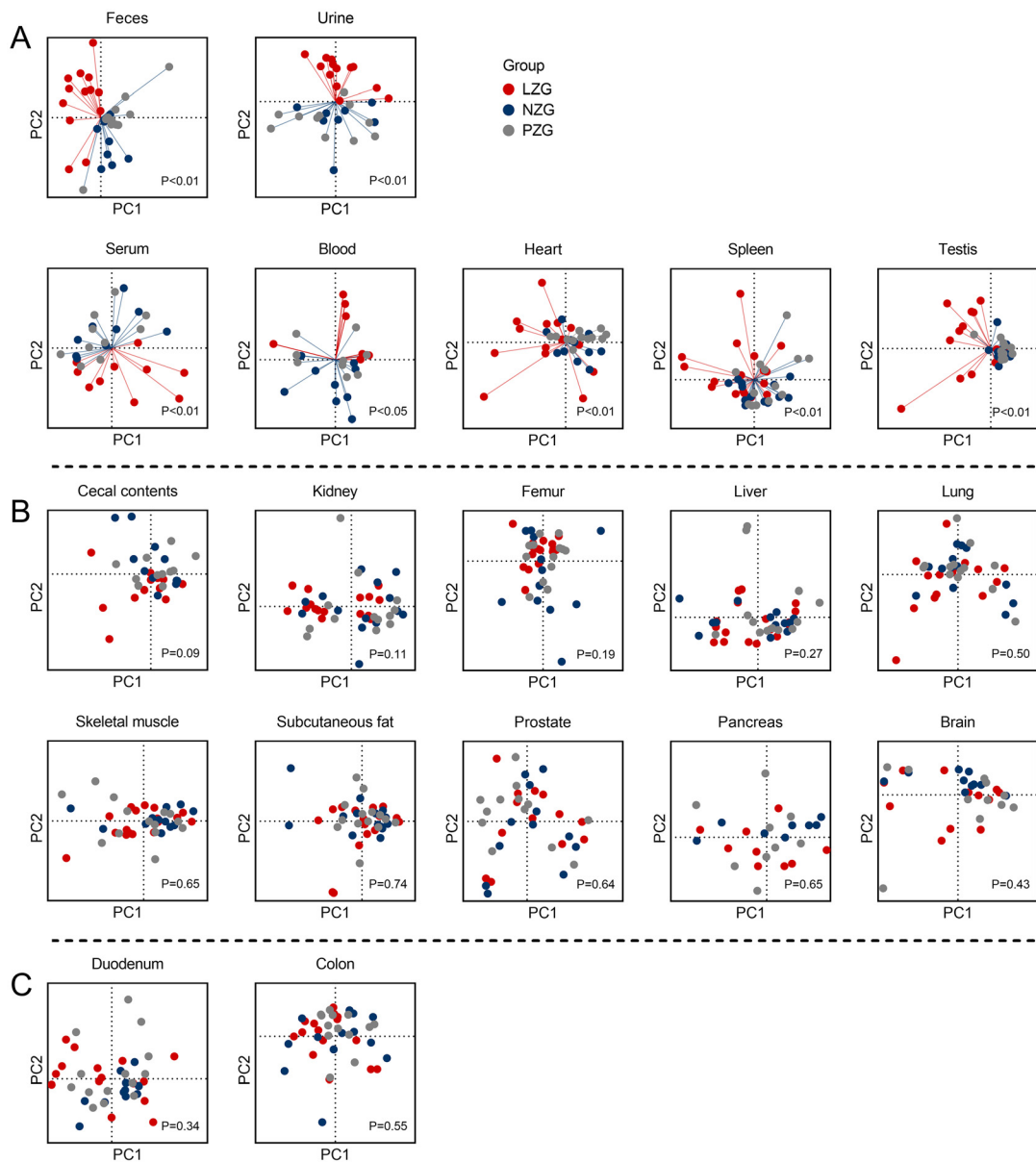


**Fig. 2** PCA score plots of nineteen different tissues and biological samples (A–C). LZG: low-zinc diet group; NZG: normal-zinc diet group; PZG: pair-fed group. Each point represents a single sample. The *p*-value from multivariate analysis of variance (MANOVA) is displayed in the lower right corner. Lines from the center to each data point are shown in (A) to indicate separation trends and highlight samples with significantly altered mineral compositions.

These findings collectively highlight the intricate relationships between tissue-specific mineral homeostasis and key biochemical parameters, underscoring the physiological significance of zinc sufficiency in maintaining metabolic balance.

## 4. Discussion

Despite the well-documented roles of zinc in growth, immune function, and metabolic regulation, the systemic impact of zinc deficiency on mineral homeostasis in the body remains poorly understood. This study addresses this gap by employing

a multi-organ ionomics approach to comprehensively investigate the impact of zinc deficiency on mineral homeostasis across multiple tissues and pathways. Our findings reveal that the disruption of mineral homeostasis in zinc-deficient rats occurs through four pathways: intake, absorption, distribution, and excretion. This integrated analysis provides novel insights into the complex physiological and metabolic consequences of zinc deficiency.

### 4.1. Organ-specific variations in mineral profiles

Previous studies have documented variations in mineral composition profiles across different organs, such as the brain,

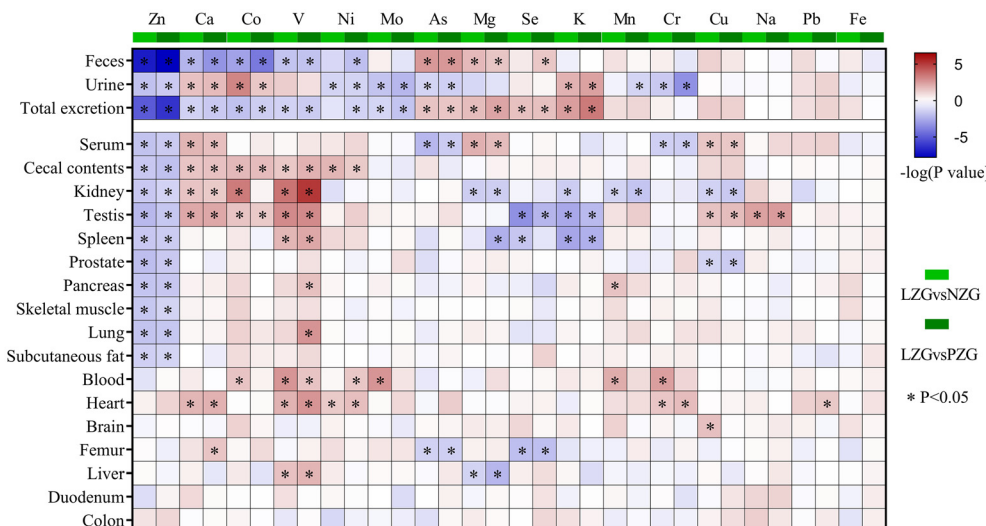


**Fig. 3** Heatmap of sixteen minerals across nineteen distinct tissues and samples. Blue: decreased concentrations in LZG; red: increased concentrations in LZG.

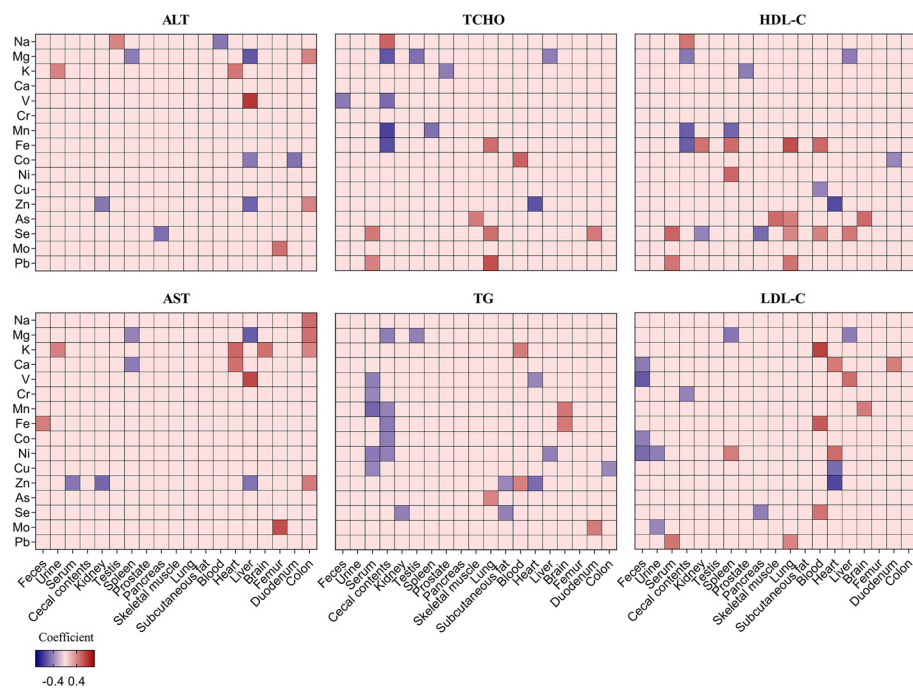


**Fig. 4** Correlation analysis between mineral concentrations and serum biochemical indicators. Blue: negative correlation; red: positive correlation.

heart, kidneys, liver, and muscles.<sup>23,24</sup> Consistent with these findings, our study extends this observation to include urine, feces, cecal contents, serum, femur, and fourteen additional organs (Fig. 1). The distinct separation in mineral composition profiles across these matrices underscores the significant heterogeneity in mineral distribution, which is likely attributable to the specific physiological functions of each organ.<sup>25</sup>

#### 4.2. Differential effects of zinc deficiency on organ-specific mineral composition profiles

Previous studies have primarily focused on changes in a limited number of mineral concentrations (usually fewer than six) induced by zinc deficiency.<sup>6-14</sup> In contrast, our study is the first to comprehensively analyze alterations in mineral composition profiles across multiple tissues and biological samples

(Fig. 2). We observed a significant difference in lifespan between the zinc-deficient and control groups. Since lifespan could also influence mineral concentrations, we performed a comparative analysis of mineral levels between deceased and surviving rats. Although some variations were observed, the overall distribution patterns of minerals in key biological samples—such as feces, urine, and serum—remained consistent across groups. The observed similarities in mineral profiles between dead and living animals suggest that the changes are likely due to zinc deficiency and not a consequence of death itself. To maintain statistical power and sample size integrity, we included data from all animals, including those that died prematurely, in the inter-group analysis. Our results demonstrate that zinc deficiency significantly alters the mineral composition of feces, urine, serum, whole blood, heart, spleen, and testis (Fig. 2A), indicating that these organs and samples are particularly sensitive to disturbances in zinc homeostasis. Conversely, mineral concentrations in the brain and intestine were minimally affected by zinc deficiency, and their mineral composition remained relatively stable. We have previously shown that mild zinc deficiency markedly alters the cardiac proteome,<sup>26</sup> whereas the brain proteome is largely unaffected.<sup>18</sup> These consistent ionomic and proteomic findings underscore tissue-specific responses to zinc deficiency and highlight the need for integrated mechanistic studies to elucidate how zinc deficiency disrupts mineral homeostasis across tissues.

#### 4.3. Four pathways of mineral homeostasis disruption

Zinc deficiency disrupts mineral homeostasis through four key pathways: reduced zinc intake, disruption of mineral absorption and excretion, and direct redistribution of certain minerals.

**4.3.1 Reduced in zinc intake.** Our results indicate no significant differences in food intake among the three rat groups at the end of the experiment (Fig. S1). However, the zinc content in the diet of the LZG was one-third that of the normal diet, the LZG received markedly less dietary zinc than the NZG and PZG (Table S26); this reduction was imposed by the diet itself. Zinc excretion in the urine and feces of these rats was also decreased, suggesting that LZG rats maintained zinc homeostasis by reducing zinc excretion. Despite this reduction, the body's zinc requirements were not met, ultimately leading to decreased zinc concentrations in serum and nine tissues (Fig. 3). Thus, low zinc intake is the primary factor contributing to reduced zinc levels in the body.

Previous studies have demonstrated that low zinc intake reduces zinc concentrations in serum, urine, feces, and several tissues, including the liver, kidneys, pancreas, prostate, testis, and intestine.<sup>7,8,11,13,27,28</sup> This study extends previous findings by reporting reduced zinc levels in the spleen, skeletal muscle, lung, subcutaneous fat, and cecal contents. However, in our study, zinc deficiency did not affect Fe concentrations in all tissues. In our previous study, we observed that a 4-week low-zinc diet led to increased iron excretion in rats.<sup>13</sup> Although the zinc content of the diets was identical in both experiments,

the key variables were the duration of the dietary intervention and the life stage of the rats—one group consisted of mature adults, while the other was elderly. Based on these observations, we hypothesize that both the duration of zinc restriction and the life stage of the animals may influence iron metabolism. Other Previous studies have shown that severe zinc deficiency (1 or 3.8 mg kg<sup>-1</sup> zinc in the diet) can increase Fe concentrations in the liver and intestines while decreasing serum Fe levels.<sup>6,7</sup> This discrepancy may be attributed to the fact that our study employed a marginal zinc-deficiency model (10 mg kg<sup>-1</sup> zinc), rather than a severe deficiency.

#### 4.3.2 Disruption of mineral absorption and excretion.

Under conditions of constant mineral intake, systemic mineral homeostasis depends primarily on the balance between absorption and excretion. Previous studies have shown that zinc deficiency affects the excretion of Ca, Se, K, and Mg.<sup>9,13,14,29</sup> In this study, we further demonstrated that zinc deficiency modulates the excretion of Co, V, Ni, Mo, and As (Fig. 3 and Table S27). Specifically, zinc deficiency reduces fecal excretion of Ca, Co, V, and Ni and urinary excretion of Mo, leading to elevated tissue concentrations in blood, heart, kidneys, testis, liver, and spleen. Conversely, it increases fecal excretion of As, Mg, and Se and urinary excretion of K, resulting in reduced tissue concentrations in kidneys, testis, spleen, femur, and liver. As shown in Fig. 5 and Table S28, the apparent absorption rates of nine minerals were differentially altered in zinc-deficient rats. Specifically, the absorption of Ca, V, Co, Ni, and Mo was elevated, whereas that of Zn, K, Mg, and Se was reduced.

Based on the above results, it can be inferred that zinc deficiency not only affects mineral excretion but also disrupts systemic mineral homeostasis by modifying absorption. It should be emphasized, however, that the observed changes in absorption were inferred based on mineral excretion levels and the apparent absorption rates. Further studies using isotope labeling techniques are needed to validate these findings. In summary, our study indicates that zinc deficiency significantly

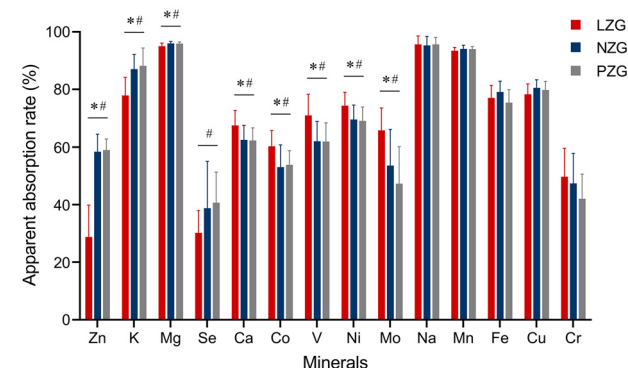


**Fig. 5** Apparent absorption rates of fourteen minerals in rats. Apparent absorption rate (%) = (mineral intake – total mineral excretion)/mineral intake × 100. LZG: low-zinc diet group; NZG: normal-zinc diet group; PZG: pair-fed group. \*:  $P < 0.05$  (LZG vs. NZG); #:  $P < 0.05$  (LZG vs. PZG).



influences both the absorption and excretion of minerals in the body.

These changes in mineral concentrations are associated with adverse health outcomes (Fig. 4). For example, alterations in the homeostasis of seven minerals (Zn, Ca, V, Ni, Mg, K and Na) in the liver, serum, kidney, heart, spleen, testis, and urine were significantly correlated with elevated serum ALT and AST levels, indicating potential liver dysfunction. Moreover, significant correlations were observed between LDL-C levels and the concentrations of six minerals (Ca, Co, V, Ni, Mo, and Mg) in the heart, liver, spleen, feces, and urine. These findings suggest that mineral imbalances induced by zinc deficiency may collectively contribute to altered lipid metabolism and metabolic dysfunction.

Notably, among all tissues examined, testicular Ca increased nearly tenfold in LZG (Table S13). Our previous work showed that zinc deficiency reduces calmodulin, elevates PTH, and subsequently alters systemic calcium distribution.<sup>30</sup> Therefore, we propose that this systemic dysregulation offers a mechanistic basis for our new finding of ectopic calcium deposition in the testes. Such changes may reduce sperm concentration and impair testicular function.<sup>31</sup>

**4.3.3 Direct redistribution of specific minerals.** Despite no observed changes in intake, absorption, or total excretion of these minerals (Mn, Cr, Cu, Na, and Pb), their tissue concentrations exhibited significant variations (Fig. 3). This suggests that zinc deficiency may primarily affect their systemic distribution, leading to tissue-specific mineral imbalances.

Exposure to Pb and Cr is associated with an increased risk of cardiovascular disease.<sup>32–34</sup> In this study, zinc-deficient rats showed elevated concentrations of Pb, Ca, V, and Ni in the heart, along with increased heart weight. Notably, cardiac Pb levels were positively correlated with heart weight (Fig. S4). In contrast, zinc supplementation has been shown to reduce the accumulation of these heavy metals and mitigate associated cardiovascular risks.<sup>35,36</sup> These findings suggest that zinc deficiency may disrupt the homeostasis of multiple metals, leading to their accumulation in the heart and potentially impairing cardiac function.

Disruptions in mineral homeostasis can lead to multi-layered physiological and metabolic disorders, contributing to the development of complex diseases. Addressing how zinc deficiency perturbs mineral homeostasis is critical for three reasons. First, although minerals are known to exhibit intricate interrelationships within the body; however, no study has yet provided objective evidence of these interactions among different mineral elements across various tissues. Second, zinc deficiency is common worldwide and has been linked to cardiovascular, skeletal and neurodegenerative disorders, but its contribution *via* systemic mineral dysregulation remains poorly quantified. Third, without a clear understanding of which minerals are altered—and in which tissues—interventions risk being poorly targeted. Our multi-organ ionomic survey now delivers the first comprehensive landscape of zinc-deficiency-induced mineral imbalances across fifteen elements, offering the essential baseline data required to

dissect the mechanistic pathways that link zinc status to organ-specific pathology.

Our findings underscore that adequate dietary zinc intake is essential for maintaining systemic mineral homeostasis. For individuals with zinc deficiency, attention must extend beyond zinc supplementation to include disturbances in other mineral levels. Zinc-rich or zinc-fortified foods are therefore critical for restoring the overall mineral imbalance induced by zinc deficiency, and their regular consumption is vital for sustaining proper mineral homeostasis.

#### 4.4. Limitation

By employing multi-organ ionomic profiling, we identified zinc-deficiency-induced disturbances in mineral homeostasis and highlighted the complex interrelationships between zinc and other minerals in the body. However, the underlying mechanisms and their potential organ-specific implications remain to be elucidated in future studies.

## 5. Conclusion

In this study, we employed a multi-organ ionomics approach to comprehensively characterize changes in mineral concentrations induced by zinc deficiency. For the first time, we found that mineral homeostasis in zinc-deficient rats is disrupted through four key pathways: intake, absorption, distribution, and excretion. This integrated perspective is essential for understanding the complex physiological mechanisms underlying zinc deficiency-related disorders. Additionally, longitudinal studies in human populations are needed to validate these findings and translate them into actionable strategies to mitigate the health impacts of zinc deficiency.

## Author contributions

Conceptualization: Maoqing Wang, Ying Li; formal analysis: Mengxu Wang, Yongzhi Sun; funding acquisition: Maoqing Wang; investigation: Mengxu Wang, Yongzhi Sun, Xinxin Gu, Yongzhu Pan, Yiwen Yang, Jingmin Tong; supervision: Maoqing Wang, Ying Li, Lan Zhao; writing – original draft: Mengxu Wang; writing – review and editing: Mengxu Wang.

## Conflicts of interest

There are no conflicts to declare.

## Data availability

The data supporting this article have been included as part of the supplementary information (SI). Supplementary information: Fig. S1: food intake of all three rat groups. Fig. S2: the urine volume and fecal weight of rats within 48 hours. Fig. S3: principal component analysis of samples and QC. Fig. S4:



heart weight and its correlation with Pb concentration in rats. Table S1: the main component of rats' diet for three groups. Table S2: concentrations of 14 minerals in low-zinc and normal diets. Table S3: linear relationships and detection limits of 16 minerals. Table S4: analytical results of standard reference material (Seronorm serum L-1 RUO,  $n = 3$ ). Table S5: spiked recoveries of 16 minerals ( $n = 6$ ). Table S6: precision of 16 minerals ( $n = 6$ ). Tables S7-S25: the concentrations of 16 minerals in the feces, urine, serum, blood, heart, spleen, testis, cecal contents, kidney, femur, liver, lung, skeletal muscle, subcutaneous fat, prostate, pancreas, brain, duodenum, and colon. Table S26: dietary and mineral intake before urine and feces collection. Table S27: 48 h total excretion of 16 minerals in rats. Table S28: apparent absorption rates of 14 minerals. See DOI: <https://doi.org/10.1039/d5fo02470f>.

## Acknowledgements

This work was supported by grants from the National Natural Science Foundation of China (82173514 and 81973036) and the Fund of Key Laboratory of Myocardial Ischemia, Ministry of Education (KF202415). We thank the Public Health Inspection Office, Heilongjiang Center for Disease Control and Prevention (Harbin, China), for providing essential facilities and technical support for mineral detection.

## References

- 1 C. Andreini, L. Banci, I. Bertini and A. Rosato, Counting the zinc-proteins encoded in the human genome, *J. Proteome Res.*, 2006, **5**, 196–201.
- 2 A. S. Prasad, Discovery of human zinc deficiency: its impact on human health and disease, *Adv. Nutr.*, 2013, **4**, 176–190.
- 3 C. T. Chasapis, P. A. Ntoupa, C. A. Spiliopoulou and M. E. Stefanidou, Recent aspects of the effects of zinc on human health, *Arch. Toxicol.*, 2020, **94**, 1443–1460.
- 4 N. M. Lowe and S. Gupta, Food fortification programmes and zinc deficiency, *Nat. Food*, 2024, **5**, 546–547.
- 5 M. Knez and J. C. R. Stangoulis, Dietary Zn deficiency, the current situation and potential solutions, *Nutr. Res. Rev.*, 2023, **36**, 199–215.
- 6 H. A. El Hendy, M. I. Yousef and N. I. Abo El-Naga, Effect of dietary zinc deficiency on hematological and biochemical parameters and concentrations of zinc, copper, and iron in growing rats, *Toxicology*, 2001, **167**, 163–170.
- 7 P. Kondaiah, R. Palika, P. Mashurabad, P. Singh Yaduvanshi, P. Sharp and R. Pullakhandam, Effect of zinc depletion/repletion on intestinal iron absorption and iron status in rats, *J. Nutr. Biochem.*, 2021, **97**, 108800.
- 8 N. H. McCormick, J. King, N. Krebs, D. I. Soybel and S. L. Kelleher, Redistribution of tissue zinc pools during lactation and dyshomeostasis during marginal zinc deficiency in mice, *J. Trace Elem. Med. Biol.*, 2015, **29**, 170–175.
- 9 F. H. Nielsen, Marginal zinc deficiency increases magnesium retention and impairs calcium utilization in rats, *Biol. Trace Elem. Res.*, 2009, **128**, 220–231.
- 10 A. K. Baltaci, H. Gokbel, R. Mogulkoc, N. Okudan, K. Ucok and I. Halifeoglu, The effects of exercise and zinc deficiency on some elements in rats, *Biol. Trace Elem. Res.*, 2010, **134**, 79–83.
- 11 S. Joshi, N. Nair and R. S. Bedwal, Dietary zinc deficiency effects dorso-lateral and ventral prostate of Wistar rats: histological, biochemical and trace element study, *Biol. Trace Elem. Res.*, 2014, **161**, 91–100.
- 12 Z. Wang, C. Peng, Y. Zhang, L. Wang, L. Yu and C. Wang, Characteristics of Zn Content and Localization, Cu-Zn SOD, and MT Levels in the Tissues of Marginally Zinc-Deficient Mice, *Biol. Trace Elem. Res.*, 2023, **201**, 262–271.
- 13 Q. Yu, X. Sun, J. Zhao, L. Zhao, Y. Chen, L. Fan, Z. Li, Y. Sun, M. Wang and F. Wang, The effects of zinc deficiency on homeostasis of twelve minerals and trace elements in the serum, feces, urine and liver of rats, *Nutr. Metab.*, 2019, **16**, 73.
- 14 R. P. Gupta, P. C. Verma, J. R. Sadana and V. K. Gupta, Effect of experimental zinc deficiency and repletion on sodium, potassium, copper and iron concentrations in guinea-pigs, *Br. J. Nutr.*, 1989, **62**, 407–414.
- 15 Y. Zhang, Y. Xu and L. Zheng, Disease Ionomics: Understanding the Role of Ions in Complex Disease, *Int. J. Mol. Sci.*, 2020, **21**, 8646.
- 16 T. Kambe, T. Tsuji, A. Hashimoto and N. Itsumura, The Physiological, Biochemical, and Molecular Roles of Zinc Transporters in Zinc Homeostasis and Metabolism, *Physiol. Rev.*, 2015, **95**, 749–784.
- 17 P. G. Reeves, Patterns of food intake and self-selection of macronutrients in rats during short-term deprivation of dietary zinc, *J. Nutr. Biochem.*, 2003, **14**, 232–243.
- 18 Y. Sun, J. Zhao, X. Song, Z. Sun, R. Zhang, J. Zhong, X. Huang, Y. Dong, Q. Yu, F. Dong, Z. Li, L. Fan, M. Wang, C. Peng and F. Wang, Effects of marginal zinc deficiency on learning and memory ability after birth, *Food Funct.*, 2022, **13**, 7204–7214.
- 19 P. Kondaiah, P. S. Yaduvanshi, P. A. Sharp and R. Pullakhandam, Iron and Zinc Homeostasis and Interactions: Does Enteric Zinc Excretion Cross-Talk with Intestinal Iron Absorption?, *Nutrients*, 2019, **11**, 1885.
- 20 B. Sandstrom, Micronutrient interactions: effects on absorption and bioavailability, *Br. J. Nutr.*, 2001, **85**(Suppl 2), S181–S185.
- 21 C. R. Williams, M. Mistry, A. M. Cherian, J. M. Williams, M. K. Naraine, C. L. Ellis, R. Mallick, A. C. Mistry, J. L. Gooch, B. Ko, H. Cai and R. S. Hoover, Zinc deficiency induces hypertension by promoting renal Na<sup>+</sup> reabsorption, *Am. J. Physiol.: Renal Physiol.*, 2019, **316**, F646–F653.
- 22 Q. Yu, J. Zhao, Y. Chen, Z. Li, Y. Sun, L. Fan, M. Wang and C.-h. Peng, Zinc deficiency decreases bone mineral density of rat by calmodulin-induced change in calcium metabolism, *bioRxiv*, 2020, DOI: [10.1101/2020.06.09.143396](https://doi.org/10.1101/2020.06.09.143396), preprint.

23 B. Zhang, D. I. Podolskiy, M. Mariotti, J. Seravalli and V. N. Gladyshev, Systematic age-, organ-, and diet-associated ionome remodeling and the development of ionomic aging clocks, *Aging Cell*, 2020, **19**, e13119.

24 J. D. Morel, L. Sauzeat, L. J. E. Goeminne, P. Jha, E. Williams, R. H. Houtkooper, R. Aebersold, J. Auwerx and V. Balter, The mouse metallomic landscape of aging and metabolism, *Nat. Commun.*, 2022, **13**, 607.

25 S. Ma, S. G. Lee, E. B. Kim, T. J. Park, A. Seluanov, V. Gorbunova, R. Buffenstein, J. Seravalli and V. N. Gladyshev, Organization of the Mammalian Ionomome According to Organ Origin, Lineage Specialization, and Longevity, *Cell Rep.*, 2015, **13**, 1319–1326.

26 Y. Sun, J. Chen, H. Wang, X. Song, Z. Sun, R. Zhang, J. Zhong, X. Gu, M. Wang, C. Peng and M. Wang, Marginal zinc deficiency alters the heart proteome of rats, *Food Funct.*, 2023, **14**, 4117–4128.

27 A. S. Prasad, D. Oberleas, P. Wolf and H. P. Horwitz, Studies on zinc deficiency: changes in trace elements and enzyme activities in tissues of zinc-deficient rats, *J. Clin. Invest.*, 1967, **46**, 549–557.

28 R. E. Burch, R. V. Williams, H. K. Hahn, M. M. Jetton and J. F. Sullivan, Serum and tissue enzyme activity and trace-element content in response to zinc deficiency in the pig, *Clin. Chem.*, 1975, **21**, 568–577.

29 T. Suzuki, K. Suzuki, J. Takahashi and Y. Nakamura, A Short-Term Zinc-Deficient Diet Maintains Serum Calcium Concentrations through Ca Absorption-Related Gene Expression in Rats, *J. Nutr. Sci. Vitaminol.*, 2024, **70**, 82–87.

30 Q. Yu, J. Zhao, Y. Chen, Z. Li, Y. Sun, L. Fan, M. Wang and C. Peng, Zinc deficiency decreases bone mineral density of rat by calmodulin-induced change in calcium metabolism, *bioRxiv*, 2020, preprint, DOI: [10.1101/2020.06.09.143396](https://doi.org/10.1101/2020.06.09.143396).

31 H. G. Wilson, B. R. Birch and R. W. Rees, Is testicular microlithiasis associated with decreased semen parameters? a systematic review, *Basic Clin. Androl.*, 2024, **34**, 23.

32 R. Chowdhury, A. Ramond, L. M. O'Keeffe, S. Shahzad, S. K. Kunutson, T. Muka, J. Gregson, P. Willeit, S. Warnakula, H. Khan, S. Chowdhury, R. Gobin, O. H. Franco and E. Di Angelantonio, Environmental toxic metal contaminants and risk of cardiovascular disease: systematic review and meta-analysis, *Br. Med. J.*, 2018, **362**, k3310.

33 Z. Pan, T. Gong and P. Liang, Heavy Metal Exposure and Cardiovascular Disease, *Circ. Res.*, 2024, **134**, 1160–1178.

34 S. Hechtenberg and D. Beyersmann, Inhibition of sarcoplasmic reticulum  $\text{Ca}^{2+}$ -ATPase activity by cadmium, lead and mercury, *Enzyme*, 1991, **45**, 109–115.

35 S. Bhattacharya, Essential Trace Metals as Countermeasure for Lead Toxicity, *J. Environ. Pathol. Toxicol. Oncol.*, 2022, **41**, 61–67.

36 M. M. Rahman, K. F. B. Hossain, S. Banik, M. T. Sikder, M. Akter, S. E. C. Bondad, M. S. Rahaman, T. Hosokawa, T. Saito and M. Kurasaki, Selenium and zinc protections against metal-(loids)-induced toxicity and disease manifestations: A review, *Ecotoxicol. Environ. Saf.*, 2019, **168**, 146–163.

